Destruction of Anderson localization by nonlinearity in kicked rotator at different effective dimensions

Destruction of Anderson localization by nonlinearity in kicked rotator at different effective dimensions

L Ermann[1] and D L Shepelyansky[2]

[1] Departamento de Física, GIyA, Comisión Nacional de Energía Atómica, Buenos Aires, Argentina
[2] Laboratoire de Physique Théorique du CNRS, IRSAMC, Université de Toulouse, UPS, 31062 Toulouse, France

E-mail: ermann@irsamc.ups-tlse.fr and dima@irsamc.ups-tlse.fr

Abstract

We study numerically the frequency modulated kicked nonlinear rotator with effective dimension $d = 1, 2, 3, 4$. We follow the time evolution of the model up to 10^9 kicks and determine the exponent α of subdiffusive spreading which changes from 0.35 to 0.5 when the dimension changes from $d = 1$ to 4. All results are obtained in a regime of relatively strong Anderson localization well below the Anderson transition point existing for $d = 3, 4$. We explain that this variation of the exponent is different from the usual $d-$ dimensional Anderson models with local nonlinearity where α drops with increasing d. We also argue that the renormalization arguments proposed by Cherroret N *et al* (arXiv:1401.1038) are not valid for this model and the Anderson model with local nonlinearity in $d = 3$.

(Some figures may appear in colour only in the online journal)

1. Introduction

At present there is a significant interest to effects of nonlinearity on Anderson localization [1]. The early theoretical and numerical studies [2, 3] have been followed by more recent and more detailed analysis performed by different groups [4–15]. The interest to this problem comes also from the side of mathematics which puts forward a fundamental question on how the pure point spectrum of Anderson localization is affected by a weak nonlinearity [16–18].

At the same time the experiments on spreading of light in nonlinear photonic lattices [19, 20] and of Bose-Einstein condensates of cold atoms in disordered potential [21] start to be able to observe effects of nonlinearity on localization.

The main effect found in numerical simulations is a subdiffusive spreading of wave packet over lattice sites induced by a moderate nonlinearity. Large time scale simulations are required to determine the spreading exponent with a good accuracy and hence the choice of a good model, that is easy for numerical simulations and at the same time captures the main physical effects, is important. One of such models is the model of kicked nonlinear rotator [2], where nonlinear phase shifts are introduced in the quantum Chirikov standard map, known also as the kicked rotator [22].

It is also important that the kicked rotator has one more interesting extension: the frequency modulated kicked rotator (FMKR) introduced in [23]. In this model the kick amplitudes are modulated with $d - 1$ incommensurate frequencies that allow one to model the Anderson transition in effective dimensions $d = 3,4$ [24–26]. This FMKR model, proposed theoretically, has been realized in skillful and impressive experiments with cold atoms by Garreau group [27]. These experiments allowed the observation of the Anderson transition in $d = 3$ and determined experimentally the critical exponents which have been found to be in agreement with analytical and numerical calculations [28]. At the moment the Garreau experiments definitely represent the most advanced experimental investigation of the Anderson transition both in fields of cold atoms and solid state disordered systems.

In a recent preprint [29] it is proposed to to study frequency modulated kicked nonlinear rotator (FMKNR) model. It is argued there that the FMKNR allows one to investigate the effects of nonlinearity of Anderson transition in $d = 3$. Here, we show that the renormalization group analysis performed in [29] is not relevant for the main physical effects leading to the nonlinearity induced wave spreading in FMKNR. However, the investigation the FMKNR model itself is interesting and provides some new information on effects of nonlinearity on Anderson localization. Thus we present here the results of our numerical studies of FMKNR in effective dimensions $d = 1, 2, 3, 4$ up to times $t = 10^9$. The model is described in section 2, numerical results are presented in section 3, simple estimates are presented in section 4 and discussion is given in section 5.

2. FMKNR model description

The time evolution of the wave function of the FMKNR is described by the equation

$$\psi(t + 1) = e^{-i(\hat{H}_0 + \hat{H}_{nl})} e^{-i\hat{V}(t)} \psi(t), \tag{1}$$

where

$$\hat{H}_0(n) = \xi_n \quad (model\ M1) \quad ; \quad \hat{H}_0(n) = Tn(n + \zeta)/2 \quad (model\ M2), \tag{2}$$

with ξ_n being random energies distributed homogeneously in the interval $-\pi, \pi$ (model $M1$) and $H_0(n) = Tn(n + \zeta)/2$ (model $M2$) are rotational phases in a kicked rotator with ζ corresponding to a quasi-momentum of Bloch waves in kicked optical lattices and parameter $T \sim \hbar_{eff} \sim 1$. Here, n is a quantum number corresponding to momentum quantization [23–28]. This part of Hamiltonian describes a free propagation

The nonlinear phase shift, as in [2], is given by

$$\hat{H}_{nl} = \beta|\psi(n)|^2, \tag{3}$$

where β is the strength on nonlinear interactions and $\psi(n)$ is taken in the momentum representation. The norm $\sum_n |\psi(n)|^2 = 1$ is conserved by unitary evolution.

The part with the kick is written in the phase representation for $\psi(\theta)$ which is conjugated to the momentum representation ($\psi(\theta + 2\pi) = \psi(\theta)$, $\hat{n} = -i\partial/\partial\theta$):

$$V(\theta, t) = k \cos\theta \left[1 + \epsilon \Pi_{i=1}^{d-1} \cos(\omega_i t) \right]. \tag{4}$$

Here, ϵ represents a strength of frequency modulation with $d - 1$ incommensurate frequencies ω_i and t is measured in a number of map iterations. For $d = 1$ in $M2$ case we obtain the usual kicked rotator [22] with $k \sim 1/\hbar_{eff}$, $T \sim \hbar_{eff}$ and the chaos parameter $K = kT = const$ ($\hbar_{eff}$ is an effective Planck constant). For $d = 2$ we use $\omega_1 = 2\pi/\lambda$, for $d = 3$ we use $\omega_1 = 2\pi/\lambda$, $\omega_2 = 2\pi/\lambda^2$. For $d = 4$ we add frequency $\omega_3 = 2\pi/\sqrt{2}$. Here $\lambda = 1.32471795724475$ is a root of cubic equation [25]. At $\beta = 0$ the models $M1$ and $M2$ manifest the phenomenon of Anderson localization in effective dimensions $d = 1, 2, 3, 4$; for $d = 3,4$ there is the Anderson transition for $k > k_c$ at a certain fixed ϵ [25–28]. For $d = 3$ the curve of the Anderson transition in the plane (k, ϵ) is analyzed in [30].

The numerical simulations of equations (1)–(4) are done by a free propagation in the momentum representation, fast Fourier transfer to the angle representation, kick in the angle representation, back Fourier transfer to the momentum representation, Then the next iteration is done in the same way. This scheme is broadly used in previous studies quoted above. Here we present our numerical results and analytical estimates. The mathematical based research of related problems of interplay of nonlinearity and Anderson localization are reviewed in [16–18].

For $\beta \sim 1$ the model $M1$ at $d = 1$ (KNR) shows a subdiffusive spreading of wave packet over sites (levels) with the second moment growth characterized by an exponent $\alpha \sim 0.4$ [2]:

$$\sigma = \sum_n |\psi(n)|^2 n^2 = \,<n^2> \,\sim t^\alpha. \tag{5}$$

It was argued [2] that this model effectively describes the spreading in discrete Anderson nonlinear Schrödinger equation (DANSE). The later studies indeed confirmed that in DANSE the exponent α is approximately the same as in the KNR [4, 7, 9]. The examples of probability spreading in the FMKNR at $d = 1, 2, 3, 4$ in the model $M1$ are shown in figure 1.

The study of the FMKNR at $d = 3$ has been proposed in [29]. At $\beta = 0$ the model FMKR can be exactly mapped on an Anderson model in effective dimension d [24, 25] by a transformation similar to those used in $d = 1$ case [31, 32]. Indeed, since the phases $\theta_i = \omega_i t$ rotates with fixed frequencies we can write the Hamiltonian in effective extended dimension d:

$$H(n, n_i, \theta, \theta_i) = H_0(n) + \sum_{i=1}^{d-1} \omega_i n_i + \beta \sum_{n_i=-\infty}^{\infty} |\psi(n, n_i)|^2 + V(\theta, \theta_i)\delta_1(t) \tag{6}$$

where $\delta_1(t)$ is a periodic delta-function with period unity, n, θ and n_i, $\theta_i (i = 1, ..., d - 1)$ are conjugated pairs of variables. Then the evolution is given by the unitary propagator:

$$\psi(n, n_i, t + 1) = \exp\left(-iH_{int}(n, n_i)\right) \exp\left(-iV(\theta, \theta_i)\right)\psi(n, n_i, t), \tag{7}$$

where $(n, n_i) = H_0(n) + \sum_{i=1}^{d-1} \omega_i n_i + \beta \sum_{n_i=-\infty}^{\infty} |\psi(n, n_i)|^2$. It is important here that the nonlinear term with β contains a sum over all additional effective dimensions $d - 1$. In a certain sense this corresponds to long-range interaction of planes in $d - 1$ dimensions. This corresponds to the physics of the FMKNR model where nonlinear coupling acts only in n independently of phases $\theta_i = \omega_i t$.
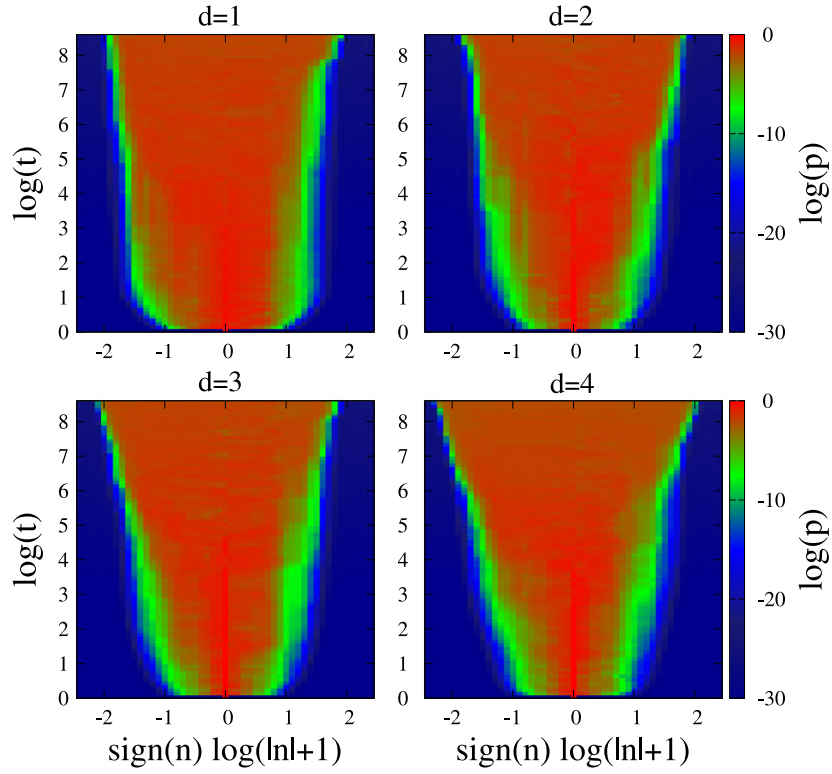
Figure 1. Time evolution of the probability spreading $p = |\psi(n)|^2$, shown by color, over momentum levels n for the model $M1$ at $k = 1.5$ ($d = 1$); $k = 0.5$, $\epsilon = 0.75$ ($d = 2, 3, 4$), and $\beta = 1$, the time interval is $1 \leqslant t \leqslant 10^9$. Initial state is $n = 0$. Probability p is shown by color variation given by color bars. The logarithms are decimal.

If we would model a real nonlinear interaction term in dimension d we would have another Hamiltonian

$$H\left(n, n_i, \theta, \theta_i\right) = H_0(n) + \sum_{i=1}^{d-1} \omega_i n_i + \beta \left|\psi(n, n_i)\right|^2 + V\left(\theta, \theta_i\right)\delta_1(t) \qquad (8)$$

where nonlinear term $\beta|\psi(n, n_i)|^2$ have no summation over n_i. Then the evolution of ψ is still given by the propagator (7) but with $H_{int}(n, n_i) = H_0(n) + \sum_{i=1}^{d-1} \omega_i n_i + \beta|\psi(n, n_i)|^2$. Such a local term appears in DANSE in $d = 2$ and has been studied in [7]. The numerical results of [7] show that the exponent α of the second moment $n^2 \propto t^\alpha$ decreases when we increase d from $d = 1$ to $d = 2$ going from $\alpha \sim 0.4$ down to $\alpha \sim 0.25$. A similar value has been also reported in numerical simulations at $d = 2$ in [33, 34]. The analytical arguments of [7] give:

$$\alpha = 2/(3d + 2). \qquad (9)$$

Of course, this expression assumes local nonlinear interaction term as in (8) that is rather different from the case of long interactions in effective dimensions effectively appearing in the FMKNR of (1), (6).

We note that equations (1)–(4) are equivalent to equations of Hamiltonian (6) since the phase shifts are linear in action variables n_i so that the corresponding phases θ_i rotate with

fixed frequencies. Also spreading in n_i does not affect spreading in n and σ. At the same time the nonlinear term in (6) drops like $1/\sqrt{\sigma}$ due to norm conservation. This is drastically different from the case of Hamiltonian (8), discussed in the renormalization group of [29], where the nonlinear term drops like $1/\sigma^{d/2}$ (see discussions in [7]).

All renormalization group arguments presented in [29] are developed for the case of local nonlinear term (8) while the numerical simulations are done for the FMKNR case (1) and (6) corresponding to the long-range interactions. Due to such a mixing of concepts the arguments of [29] are not valid. Also, we point out that the renormalization group arguments [29] assume a proximity to a critical point of the Anderson transition. But all the studies of the nonlinearity induced destruction of Anderson localization show that it takes place even in a relatively strong localization regime and also in $d = 1,2$ where the Anderson transition is absent and linear waves are always localized. Due to those reasons we argue that the approach of [29] is not applicable for the physics of phenomenon of DANSE. However, the investigation of the FMKNR model at certain d is interesting and thus we present our results below for $d = 1, 2, 3, 4$.

3. Numerical results

In our numerical studies we fix $k = 1.5$ for $d = 1$ and $k = 0.5$, $\epsilon = 0.75$ for $d = 2, 3, 4$ for both models $M1$ and $M2$. The frequencies ω_i are fixed at values given in the previous Section. For the model $M2$ we use $T = 2.89$ as in experiments [29]; we use up to 10 random values of quasi-momentum ζ in model $M2$ ($0 \leqslant \zeta < 1$) and up to 10 disorder realizations in model $M1$. The initial state is taken at $n = 0$. The transition between momentum and angle representations is done by the fast Fourier transform.

For $d = 3,4$ we find that both models have approximately the same critical value k_c of Anderson transition. For $d = 3$ we have $k_c \approx 1.8$ in agreement with [25, 26]. Also for $d = 4$ both models have the same critical point $k_c \approx 1.15$ at $\epsilon = 0.9$ and $k_c \approx 1.3$ at $\epsilon = 0.75$. At $d - 1$ frequencies the classical chaos border becomes very small in k so that random rotational phases in model $M1$ have the Anderson transition approximately at the same point as in the model $M2$. We stress that all amplitudes of k used in our simulations are located in a well localized phase being rather far from the Anderson transition in $d = 3,4$. At those k values the localization length $\ell \sim 1 - 2$ captures only a couple of sites (see figures 1,9 in [25]).

The spearing of probability $p_n = |\psi(n)|^2$ over momentum modes n is shown as a function of time $t \leqslant 10^9$ in figure 1 for model $M1$. The data show that $|\psi(n)|^2$ spreads more or less homogeneously over a plateau (chapeau) which width increases with time.

The growth of the second moment σ with time $t \leqslant 10^9$ is shown in figure 2 for models $M1$ and $M2$ for a one disorder realization in $M1$ and one value of quasi-momentum in model $M2$ (a random value in the interval $0 \leqslant \zeta < 1$).

We also determine the dependence $\sigma(t)$ for $1 \leqslant t \leqslant 10^8$ for both models for 10 realizations of disorder ($M1$) or 10 random values of ζ ($M2$). The values of exponent α are shown in figure 3 for all four dimensions d. Averaging over these 10 values of α we find the average α value and its error-bar. For model $M1$ we obtain $\alpha = 0.36 \pm 0.02$, 0.45 ± 0.03, 0.50 ± 0.04, 0.52 ± 0.04 and for model $M2$ we obtain $\alpha = 0.35 \pm 0.03$, 0.43 ± 0.03, 0.51 ± 0.03, 0.54 ± 0.04 respectively for $d = 1, 2, 3, 4$. Within the error-bars both models have the same value of α for a given dimension.

We point out that for one disorder realization there are fluctuations in the growth of σ well visible in figure 2 giving up and down fluctuations of a local slope of growth. This is an example of fluctuations typical for mesoscopic disordered systems. However, after averaging
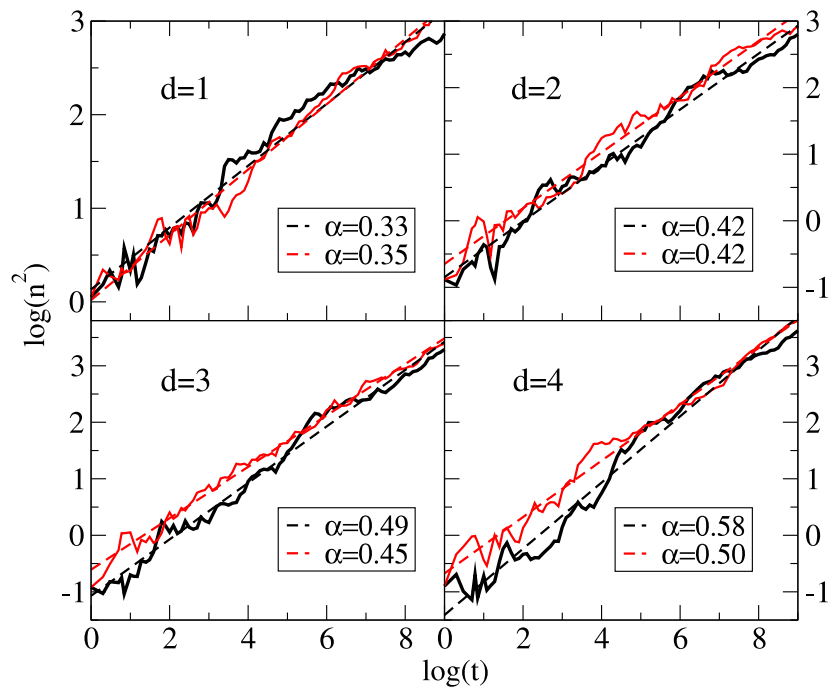
Figure 2. Dependence of the second moment $\sigma \equiv \langle n^2 \rangle$ of probability distribution on time t shown in logarithmic scale for models $M1$ (black) and $M2$ (red) with dimensions $d = 1, 2, 3, 4$. Parameters k, ϵ, β are as in figure 1 and $T = 2.89$ for $M2$. The power law fit of subdiffusive spreading $\sigma \sim t^{\alpha}$ is shown by the straight dashed lines for each model. Effective dimensions d and fitted values of α are shown in each panel, logarithms are decimal.
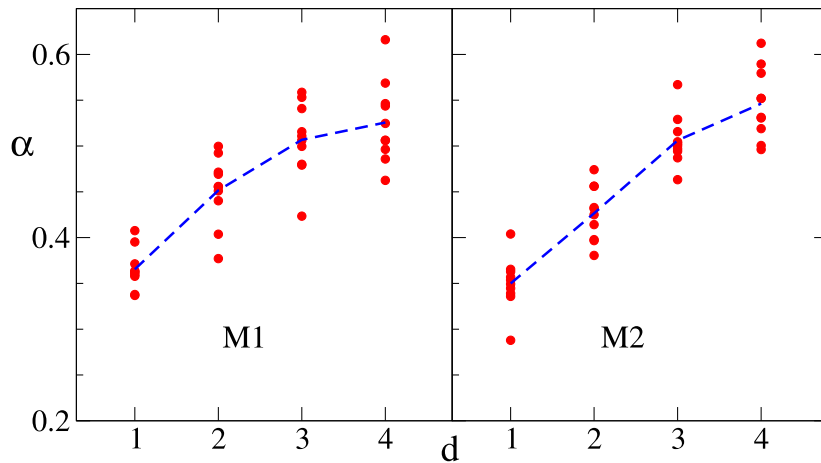

Figure 3. The subdiffusive spreading exponent α for dimensions $d = 1, 2, 3, 4$ of both models. The model parameters are as in figures 1, 2. The exponents α are computed up to time $t = 10^8$ for 10 random realizations of disorder in model $M1$ and 10 random values of quasi-momentum ζ in model $M2$ (left and right panels respectively). Dashed blue curves represent average α dependence on dimension d for each model.

over 10 realizations we obtain the accuracy of the exponent α on a level of 6% while the variation of α with d represents about 50% being well outside of statistical errors. Also the numerical results presented in [7, 9] confirm that the exponent α is independent of time for $d = 1$.

We note that the case $d = 3$ for model $M2$ has been studied in [29] with numerically obtained value $\alpha \approx 0.4$. However, the time scales considered there are about 1000 times smaller than those considered here. Also in [29] the working point was placed rather close to the Anderson transition so that the localization length of linear problem was rather large so that it was more difficult to reach the asymptotic regime (in our case we are far from the Anderson transition point and $\ell \sim 1 - 2$). As we see the exponent α is not significantly affected by such a large change of localization length of a linear problem, thus clearly indicating that the theoretical renormalization arguments of [29] are not relevant for FMKNR and the Anderson model with nonlinearity in $d = 3$ (the independence of α of localization length has been discussed by different groups for $d = 1$, see e.g. [4, 7, 9]).

Our data show a clear tendency of growth of α with d in the FMKNR model (1). Of course, this dependence is absolutely different from the one of (9) obtained for a local nonlinear term.

4. Simple estimates

It is interesting to note that the exponent $\alpha = 1/2$ corresponds to a so-called regime of 'strong chaos' [9, 10, 35]. Indeed, the numerical simulations performed in [9, 10] introduced a randomization of phases of linear eigenmodes after a fixed time scale $\tau \sim 1$ showing numerically that in such a case $\alpha = 1/2$. This relation can be understood on a basis of simple estimates in the following way: the equations of amplitudes of linear modes C_m in the interaction representation have a form $i\partial C/\partial t \sim \beta C^3$ [2, 4, 7]. In [2, 4, 7] it was assumed that there is a plateau in amplitudes of $C \sim 1/(\Delta n)^{1/2}$ with $|m| < \Delta n$ and $C = 0$ outside of the plateau. Then the time scale t_s after which a next level outside of plateau will be populated is estimated as $\Gamma \sim 1/t_s \sim \beta^2 C^6 \sim \beta^2/(\Delta n)^3$ due to norm conservation. Since the diffusion coefficient is $D \sim (\Delta n)^2/t \sim \Gamma$ this gives $\alpha = 2/5$ for $(d = 1)$ and the relation (9) for any d [2, 7].

It is also possible to assume that there is a certain smooth profile distribution of C values on the plateau and use the estimate of the Fermi golden rule type [36] used in quantum mechanics with $\Gamma \sim \beta^2 C^4 \sim \beta^2/(\Delta n)^2$ that would lead to $\alpha = 1/2$ and $\sigma \sim t^{1/2}$ in agreement with arguments of [9, 10, 35]. This assumes random phase approximation and mixing of phases on a certain fixed time scale τ. Thus in such a case we can write

$$(\Delta n)^2 \sim (t/\tau)^{1/2}. \tag{10}$$

However, it is clear that the time scale should grow with Δn since the rate of chaotization should become smaller and smaller with time since the nonlinear term decreases. The most natural assumption is that $\tau \sim 1/\delta\omega \sim \Delta n$ where $\delta\omega \sim \beta|\psi_n|^2$ is a nonlinear frequency shift. Thus using the relation $\tau \sim \Delta n$ we obtain from (10) that again $\alpha = 2/5$.

The numerically obtained values of α (see figure 3) are approximately located in the range $0.35 \leqslant \alpha \leqslant 0.5$. It is possible that for $d = 3,4$ a larger number of modulation phases generates a more dense spectrum which is more similar to random phase approximation with $\tau \sim const$ corresponding to the strong chaos regime with $\alpha = 1/2$. It is also possible that times even longer than $t = 10^9$ are required to be in a really asymptotic regime.

5. Discussion

We present the results of numerical studies of the FMKNR models with nonlinearity in effective dimensions $d = 1, 2, 3, 4$. Our results show that the exponent α of subdiffusive spreading increases from $\alpha \approx 0.35$ up to $\alpha \approx 0.5$ when d changes from 1 to 4. We show that this dependence on d corresponds to a regime of nonlinearity with a long-range interactions typical for FMKNR. In contrast to FMKNR, for Anderson models, with local nonlinearity like for DANSE [4, 7], we have a decrease of the exponent α with increase of d given by the relation (9).

In our opinion, the exact derivation of the expression for the exponent α represents a nontrivial problem, Indeed, the results presented in [13] clearly show that the measure of chaos decreases with a growing system size. This important result leads us to a conclusion that a spreading proceeds over more and more tiny chaotic layers of smaller and smaller measure. In such a regime a role of correlations should be important and exact derivation of the expression for α requires additional information about a structure of chaotic layers in many-body nonlinear systems.

We note that, after the submission of our paper to *J. Phys.* A: *Math. Theor.* and arXiv: 1403.2692, the paper [29] has been published in a journal with the statement of the authors of [29] that 'our disorder theory (3) is strictly speaking not directly applicable to the QPKNR [equations (1–4) here]] which pertains to a 1D configuration space ... we expect this difference to be crucial for a precise determination of the subdiffusion exponent...'.

References

[1] Anderson P W 1958 *Phys. Rev.* **109** 1492
[2] Shepelyansky D L 1993 *Phys. Rev. Lett.* **70** 1787
[3] Molina M I 1998 *Phys. Rev.* B **58** 12547
[4] Pikovsky A S and Shepelyansky D L 2008 *Phys. Rev. Lett.* **100** 094101
[5] Flach S, Krimer D O and Skokos C 2009 *Phys. Rev. Lett.* **102** 024101
[6] Skokos C, Krimer D O, Komineas S and Flach S 2009 *Phys. Rev.* E **79** 056211
[7] Garcia-Mata I and Shepelyansky D L 2009 *Phys. Rev.* E **79** 026205
[8] Skokos C and Flach S 2010 *Phys. Rev.* E **82** 016208
[9] Lapteva T V, Bodyfelt J D, Krimer D O, Skokos C and Flach S 2010 *Europhys. Lett.* **91** 30001
[10] Bodyfelt J D, Lapteva T V, Skokos C, Krimer D O and Flach S 2011 *Phys. Rev.* E **84** 016205
[11] Johansson M, Kopidakis G and Aubry S 2010 *Europhys. Lett.* **91** 50001
[12] Mulansky M and Pikovsky A 2010 *Europhys. Lett.* **90** 10015
[13] Pikovsky A and Fishman S 2011 *Phys. Rev.* E **83** 025201
[14] Mulansky M and Pikovsky A 2013 *New. J. Phys.* **15** 053015
[15] Skokos C, Gkolias I and Flach S 2013 *Phys. Rev. Lett.* **111** 064101
[16] Wang W-M and Zang Z 2008 arXiv:0805.3520
[17] Bourgain J and Wang W-M 2008 *J. Eur. Math. Soc.* **10** 1
[18] Fishman S, Krivolapov Y and Soffer A 2012 *Nonlinearity* **25** R53
[19] Schwartz T, Bartal G, Fishman S and Segev M 2007 *Nature* **446** 52
[20] Lahini Y, Avidan A, Pozzi F, Sorel M, Morandotti R, Chirstodoulis D N and Silberberg Y 2008 *Phys. Rev. Lett.* **100** 013906
[21] Lucioni E, Deissler B, Roati G, Zaccanti M, Moduggno M, Larcher M, Dalfovo F, Inguscio M and Modugno G 2011 *Phys. Rev. Lett.* **106** 230403
[22] Chirikov B V, Izrailev F M and Shepelyansky D L 1981 *Math. Phys. Rev.* (*Sov. Scient Rev. C-Math Phys. Rev.* 2) ed S P Novikov (Chur, Switzerland: Harwood Academic) 209
[23] Shepelyansky D L 1983 *Physica* D **8** 208
[24] Casati G, Guarneri I and Shepelyansky D L 1989 *Phys. Rev. Lett.* **62** 345
[25] Borgonovi F and Shepelyansky D L 1996 *J. de Physique I France* **6** 287
[26] Shepelyansky D L 2011 arXiv:102.4450 [cond-mat.dis-nn]

[27] Chabé J, Lemarié G, Grémaud B, Delande D, Sziftgiser P and Garreau J C 2008 *Phys. Rev. Lett.* **101** 255702

[28] Lopez M, Clément J-F, Sziftgiser P, Garreau J C and Delande D 2012 *Phys. Rev. Lett.* **108** 095701

[29] Cherroret N, Vermersch B, Garreau J C and Delande D 2014 *Phys. Rev. Lett.* **112** 170603 (arXiv:1401.1038 [cond-mat.dis-nn])

[30] Lopez M, Clément J-F, Lemarié G, Delande D, Szriftgiser P and Garreau J C 2013 *New. J. Phys.* **15** 065013

[31] Fishman S, Grempel D R and Prange R E 1982 *Phys. Rev. Lett.* **49** 509

[32] Shepelyansky D L 1987 *Physica* D **28** 103

[33] Laptyeva T V, Bodyfelt J D and Flach S 2012 *Eurphys. Lett.* **98** 60002

[34] Gligoric G, Rayanov K and Flach S 2013 *Eurphys. Lett.* **101** 10011

[35] Basko D 2014 *Phys. Rev.* E **89** 022921

[36] Landau L D and Lifshitz E M 1974 *Quantum Mechanics (Non-relativistic Theory)* (in Russian: Nauka, Moskva)